JACS
JOURNAL OF THE AMERICAN CHEMICAL SOCIETY

Communication

pubs.acs.org/JACS

Unravelling the Impact of Reaction Paths on Mechanical Degradation of Intercalation Cathodes for Lithium-Ion Batteries

Juchuan Li,[†] Qinglin Zhang,[‡,§] Xingcheng Xiao,[*,‡] Yang-Tse Cheng,[§] Chengdu Liang,[∥] and Nancy J. Dudney[*,†]

[†]Materials Science and Technology Division and [∥]Center for Nanophase Materials Sciences, Oak Ridge National Laboratory, Oak Ridge, Tennessee 37831, United States

[‡]Chemical and Materials Systems Laboratory, General Motors Research and Development Center, Warren, Michigan 48090, United States

[§]Department of Chemical and Materials Engineering, University of Kentucky, Lexington, Kentucky 40506, United States

Supporting Information

ABSTRACT: The intercalation compounds are generally considered as ideal electrode materials for lithium-ion batteries thanks to their minimum volume expansion and fast lithium ion diffusion. However, cracking still occurs in those compounds and has been identified as one of the critical issues responsible for their capacity decay and short cycle life, although the diffusion-induced stress and volume expansion are much smaller than those in alloying-type electrodes. Here, we designed a thin-film model system that enables us to tailor the cation ordering in $LiNi_{0.5}Mn_{1.5}O_4$ spinels and correlate the stress patterns, phase evolution, and cycle performances. Surprisingly, we found that distinct reaction paths cause negligible difference in the overall stress patterns but significantly different cracking behaviors and cycling performances: 95% capacity retention for disordered $LiNi_{0.5}Mn_{1.5}O_4$ and 48% capacity retention for ordered $LiNi_{0.5}Mn_{1.5}O_4$ after 2000 cycles. We were able to pinpoint that the extended solid-solution region with suppressed phase transformation attributed to the superior electrochemical performance of disordered spinel. This work envisions a strategy for rationally designing stable cathodes for lithium-ion batteries through engineering the atomic structure that extends the solid-solution region and suppresses phase transformation.

Long-lasting lithium-ion batteries are one of the key enabling technologies for electric vehicles and electrochemical stationary energy storage. The desired ultralong lifetime (service life >10 years and >5000 cycles) poses a grand challenge to the intrinsic stability of battery electrodes. Without understanding the fundamental structural and chemical properties of cathodes, we cannot rationally design or optimize electrode materials. In many cases, lithium-ion battery electrodes suffocate after repetitive charge−discharge (lithium extraction−insertion) cycles because of irreversible electrochemical reactions and/or mechanical degradation. While identifying irreversible electrochemical reactions is straightforward, mechanical degradation caused by volume change and the associated stress are still puzzling researchers. Large volume change (up to ∼300%) in alloying- and conversion-type anodes, such as silicon and tin oxide, has been identified as the primary cause of their short cycle life.[1] A myriad of studies proved that mechanical degradation as a failure mode can be eliminated by suppressing the volume change[2,3] and lowering the stress/strain[2,4,5] through various strategies including limiting the capacity,[6] adding inactive buffer components,[7,8] engineering nanostructures,[9−11] and introducing mechanical clamping layers.[1] Following this logic, mechanical failure should not be a concern for intercalation-type cathodes, since the volume change upon cycling is only 2−7%,[12,13] much smaller than that in alloying-type anodes which is typically >100%. In apparent contradiction, cracking as a failure mode has been observed for many intercalation-type cathodes, including layered $LiCoO_2$[14] and $LiNiO_2$[15] and spinel-type $LiMn_2O_4$.[16] While the cycle life of most cathodes is limited to hundreds of cycles even in half-cells with an inexhaustible supply of electrolyte and lithium, $LiFePO_4$, whose volume expansion is >6.6%,[17] is capable of delivering an extremely long life of tens of thousands cycles.[18,19] These inconsistencies point to the need to understand the fundamental cause for the mechanical degradation of intercalation-type cathodes.

It is not easy to identify the intrinsic cause for degradation in a given cathode material, because the actual failure modes of lithium-ion batteries are usually on a complex basis. Chemical composition, phase and structural purity, electrochemical reaction paths, and microstrain and stress during cycling are generally considered intrinsic factors affecting the cycling life of cathodes. However, the actual performance of composite electrodes is also a function of the necessary inactive components, including binders and conducting additives as well as fabrication procedures such as coating and calendaring.[20,21] Furthermore, possible side reactions between the electrolyte and the current collectors and cell hardware further complicate the analysis.[22,23] The above factors bring complication to access the stability for the active material. For example, although some works show that ordered $LiNi_{0.5}Mn_{1.5}O_4$ possesses inferior stability compared to the disordered spinel,[24,25] under certain conditions, ordered $LiNi_{0.5}Mn_{1.5}O_4$ is capable of delivering excellent cycle life.[26] While many of these

Received: June 19, 2015
Published: October 18, 2015

DOI: 10.1021/jacs.5b06178
J. Am. Chem. Soc. 2015, 137, 13732−13735

problems can be addressed through engineering efforts, the scientific reasons for mechanical degradation of intercalation-type cathodes are generally overshadowed by these superficial phenomena. A clean model system with side-by-side comparison is required to illuminate the intrinsic degradation mechanisms of intercalation-type cathode materials.

Here by comparing two model cathodes, disordered and ordered $LiNi_{0.5}Mn_{1.5}O_4$ high-voltage spinel, we demonstrate how a subtle structural difference in cathodes impacts the reaction routes, leading to significantly different cycling performance. These two cathodes are chosen as a model system for this study because they possess the same chemical composition and similar lattice structures, except for cation ordering where Ni and Mn occupy distinct crystallographic sites in ordered $LiNi_{0.5}Mn_{1.5}O_4$ and are randomly located in disordered $LiNi_{0.5}Mn_{1.5}O_4$ (see Figure S1 and related discussion). In order to measure the intrinsic performance of these two materials without interference from the polymer binder and additives as in conventional composite electrodes, we successfully synthesized these two cathodes in the form of thin films through sputtering. In addition, they have the same surface areas and thickness (1 μm), which allows for a more direct comparison of the two cathodes. The stress in cathodes during electrochemical cycling is quantified in situ using a multibeam optical stress sensor (MOSS) with a customized electrochemical cell (Scheme. S1). We show that different phase evolution paths of the cathodes cause a slight change in the stress patterns and a huge difference in cycle life.

Disordered and ordered $LiNi_{0.5}Mn_{1.5}O_4$ show distinct long-term cycling performance, although they have very similar chemical composition and structure. The morphology and crystal structures of disordered ($Fd\bar{3}m$) and ordered ($P4_332$) $LiNi_{0.5}Mn_{1.5}O_4$ film cathodes are confirmed by SEM, XRD, FTIR, and Raman spectroscopy (Figures S2–S5). Furthermore, the lack of evidence for Mn^{3+} in XPS and differential capacity results reveals no oxygen deficiency in disordered $LiNi_{0.5}Mn_{1.5}O_4$ (Figure S6–S7). In order to investigate the cycle life of cathodes independent of the depletion of electrolyte with aging,[27] the measurement is performed in half cells with ample electrolyte and lithium. In most cases, the degree of disordering in $LiNi_{0.5}Mn_{1.5}O_4$ powders is inevitably coupled with oxygen content during annealing.[28,29] With thin-film cathodes produced by sputtering, it is possible to decouple these two factors and fabricate disordered $LiNi_{0.5}Mn_{1.5}O_4$ with stoichiometric oxygen content (see Figures S6–S8 and discussion). As shown in Figure 1, disordered $LiNi_{0.5}Mn_{1.5}O_4$ delivers very stable capacity upon cycling after initial stabilization with an average retention of about 99.997% per cycle. As a result, 116 mAh/g, corresponding to 95% of the total available capacity, is usable after an extended cycling of 2000 charge–discharge cycles. The voltage-capacity profiles and the two plateaus corresponding to $Ni^{2+/3+/4+}$ redox are well retained during cycling, as shown in Figure 1B (also see Figure S8 for dq/dV plots). These facts prove that disordered $LiNi_{0.5}Mn_{1.5}O_4$ has a superior structural stability that enables ultralong cycle life. In contrast, after initial stabilization the capacity retention of ordered $LiNi_{0.5}Mn_{1.5}O_4$ is only 99.96% per cycle, leading to a considerable decay in capacity upon extended cycling. As a result, capacity in ordered $LiNi_{0.5}Mn_{1.5}O_4$ decreases to 80% of the initial value after ~900 cycles, and only 57 mAh/g (48%) is retained after 2000 cycles.

As it turns out, the distinct cycling performance corresponds to the cracking in $LiNi_{0.5}Mn_{1.5}O_4$ cathodes. We compare the surface morphology of pristine and post-cycling $LiNi_{0.5}Mn_{1.5}O_4$ spinel, as shown in Figure 2. Ordered $LiNi_{0.5}Mn_{1.5}O_4$ shows high crack

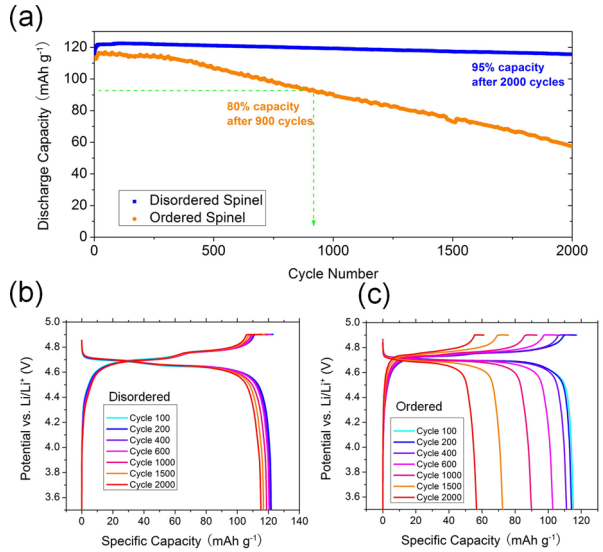

Figure 1. Cycling performance of disordered and ordered $LiNi_{0.5}Mn_{1.5}O_4$. (a) Long-term capacity retention of disordered and ordered $LiNi_{0.5}Mn_{1.5}O_4$. (b) Voltage–capacity profiles of disordered $LiNi_{0.5}Mn_{1.5}O_4$. (c) Voltage–capacity profiles of ordered $LiNi_{0.5}Mn_{1.5}O_4$.

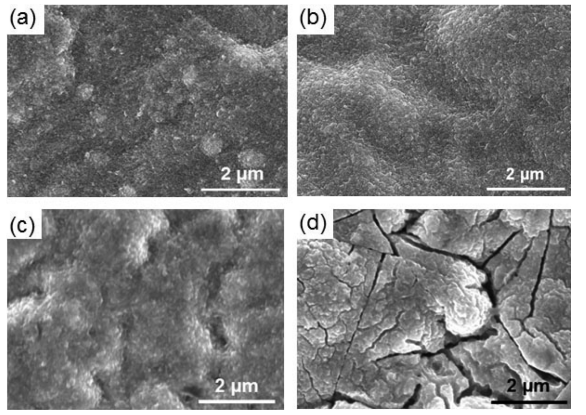

Figure 2. Surface morphology of (a) disordered and (b) ordered $LiNi_{0.5}Mn_{1.5}O_4$ before electrochemical cycling. (c) Surface morphology of disordered $LiNi_{0.5}Mn_{1.5}O_4$ after 2000 cycles. (d) Cracking formed in ordered $LiNi_{0.5}Mn_{1.5}O_4$ after 2000 cycles.

density after 2000 cycles, including long, straight primary cracks and short secondary cracks. Interconnected cracks as a result of electrochemical cycling leads to loss of electrical contact of active materials by severe peeling off of thin-film electrodes. Partial exposure of the Pt current collector is shown in Figure S9. In comparison, no sign of cracking is detected in disordered $LiNi_{0.5}Mn_{1.5}O_4$ after 2000 charge–discharge cycles (Figure 2C). It is worth noting that the thickness for both $LiNi_{0.5}Mn_{1.5}O_4$ films is smaller than 2 μm, which is believed a critical thickness for severe cracking in initial cycles.[30] Thus, the cracking behavior in Figure 2 reveals the fatigue failure of $LiNi_{0.5}Mn_{1.5}O_4$ cathodes caused by subcritical stresses. Disordered and ordered $LiNi_{0.5}Mn_{1.5}O_4$ in this work have the same chemical composition and surface chemistry, very similar structures and grain size; more importantly, they are of the same thickness[30] and experience identical volume change (6.2%) upon lithium extraction and insertion.[28] What is causing this unexpected markedly different cracking behavior?

DOI: 10.1021/jacs.5b06178
J. Am. Chem. Soc. 2015, 137, 13732–13735

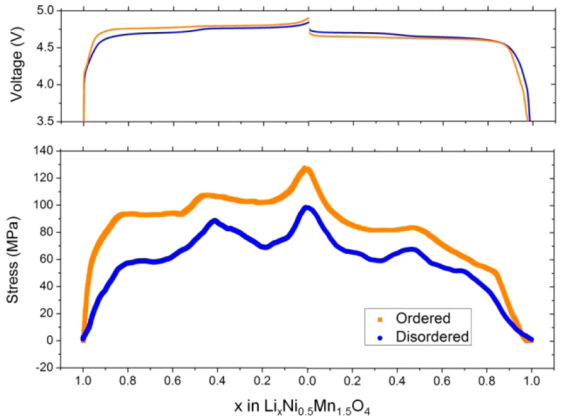

Figure 3. Stress evolution in $LiNi_{0.5}Mn_{1.5}O_4$ during cycling. The corresponding voltage profiles are shown in the upper panel.

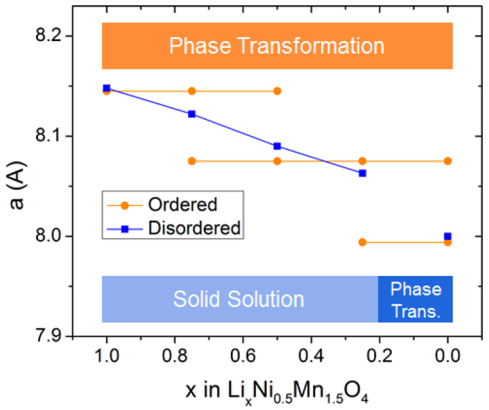

Figure 4. Lattice parameter of $Li_xNi_{0.5}Mn_{1.5}O_4$ with different lithium contents. The lattice parameter is determined by XRD of (311) and (400) planes.

It is instructive to compare the stress of both cathode materials upon lithium extraction and insertion. We use the in situ electrochemical stress sensor to monitor the stress evolution in these two $LiNi_{0.5}Mn_{1.5}O_4$ cathodes during electrochemical cycling. Directly measuring the stress in composite electrodes is very challenging, and successful synthesis of thin-film cathodes enables the direct quantification of stress. Stress measurement is repeated with three samples for each $LiNi_{0.5}Mn_{1.5}O_4$, and the representative stress evolution is shown in Figure 3. During the charging process, lithium is extracted from the $LiNi_{0.5}Mn_{1.5}O_4$ lattice, causing the volume to shrink.[31,32] This reduction in volume gives rise to tensile stress in $LiNi_{0.5}Mn_{1.5}O_4$, as shown in Figure 3. Tensile stresses in both cathodes increase with charging and relaxes partially at 50% state of charge. Upon the reverse Li insertion, the tensile stresses relax fully back to the original state. The partial relaxation of stress and the stress pattern might be related with local cation ordering and Li-vacancy configuration in $LiNi_{0.5}Mn_{1.5}O_4$.[33,34] The maximum average stress is 98 MPa in disordered $LiNi_{0.5}Mn_{1.5}O_4$ and 126 MPa in ordered $LiNi_{0.5}Mn_{1.5}O_4$. These stress values are much smaller than the values for silicon anodes[35] and are even smaller than that in graphite anodes (~250 MPa),[36] the most widely used commercial anodes. Further considering the fact that volume change in $LiNi_{0.5}Mn_{1.5}O_4$ is smaller than that in $LiFePO_4$, such a small difference in the stress of disordered and ordered $LiNi_{0.5}Mn_{1.5}O_4$ is not likely a clear indication of their distinct cycling performance. However, the stress patterns are slightly different, indicating possible different reaction paths in disordered and ordered $LiNi_{0.5}Mn_{1.5}O_4$.

The reaction paths in disordered and ordered $LiNi_{0.5}Mn_{1.5}O_4$ are revealed by ex situ XRD measurements. Ordered $LiNi_{0.5}Mn_{1.5}O_4$ undergoes multiple first-order phase transformations upon Li insertion and extraction, as confirmed by the lattice parameter changes in Figure 4 extracted from XRD (Figure S8):

$$LiNi_{0.5}Mn_{1.5}O_4\ (I) \xrightarrow{\text{phase trans.}} Li_{0.5}Ni_{0.5}Mn_{1.5}O_4\ (II) \xrightarrow{\text{phase trans.}} Ni_{0.5}Mn_{1.5}O_4\ (III)$$

During charging, Phase II appears before the overall composition reaches $Li_{0.75}Ni_{0.5}Mn_{1.5}O_4$ and exists upon the full removal of lithium from the lattice. The final phase III $Ni_{0.5}Mn_{1.5}O_4$ appears before the overall composition reaches $Li_{0.25}Ni_{0.5}Mn_{1.5}O_4$. These facts indicate that the ordered $LiNi_{0.5}Mn_{1.5}O_4$ undergoes phase transformations during cycling, the traditionally believed reaction route for intercalation cathodes. On the other hand, disordered $LiNi_{0.5}Mn_{1.5}O_4$ follows a single-phase solid-solution reaction route upon Li extraction, rather than phase transformation, before the end of charging:

$$LiNi_{0.5}Mn_{1.5}O_4\ (I) \xrightarrow{\text{solid solu.}} Li_{0.25}Ni_{0.5}Mn_{1.5}O_4\ (I) \xrightarrow{\text{phase trans.}} Ni_{0.5}Mn_{1.5}O_4\ (III)$$

The change in lattice parameter of the last phase is related with rearrangement of atoms and associated relaxation processes. Contrary to some previous reports,[24,37] our results show that the last phase $Ni_{0.5}Mn_{1.5}O_4$ does not form until the very end of lithium extraction. In other words, at most times during electrochemical cycling, disordered $LiNi_{0.5}Mn_{1.5}O_4$ undergoes a smooth, single-phase solid-solution reaction but not phase transformation.

Stress in $LiNi_{0.5}Mn_{1.5}O_4$ cathode is caused by volume change and phase evolution. For disordered $Li_xNi_{0.5}Mn_{1.5}O_4$, the solid-solution reaction in the composition range $0.2 < x < 1$ leads to a seamless reaction, and the concentration gradient is mainly responsible for the stress observed in Figure 3. However, for ordered $LiNi_{0.5}Mn_{1.5}O_4$, the topotactic phase transformation involving rearrangement of atoms leads to abrupt changes in lattice parameters at phase boundaries, adding additional stress. We expect that the local stress at phase boundaries, which are possible crack initiation sites, is much higher than the average value measured for the electrode. Considering the fact that the two cathodes in this work process the same chemical composition, thickness, and similar grain size, phase evolution behavior and reaction paths are the only possible causes for their distinct cycling performance.

It is generally believed that lithium diffusion-induced stress is directly responsible for cracking in battery electrodes once it exceeds the fracture strength of the electrode materials. However, our results show that stress is only a superficial indicator, and the fundamental cause for cracking lies in reaction pathways. In the case of phase transformations, the localized stress around the phase boundaries could easily lead to crack nucleation and propagation, since the defect density along the boundary is much higher than that in the bulk.[38] In contrast, the stress can be homogenized and uniformly distributed in the bulk of the cathode materials in the scenario of a solid-solution reaction. It has been predicted recently that the phase evolution path in $LiNi_{0.5}Mn_{1.5}O_4$ strongly depends on the degree of Ni–Mn cation ordering.[34] With completely random Ni/Mn distribution, it is possible to extend the solid-solution region over the entire composition range at ambient temperature. It has been reported that ordered $LiNi_{0.5}Mn_{1.5}O_4$ exhibits excellent

DOI: 10.1021/jacs.5b06178
J. Am. Chem. Soc. 2015, 137, 13732–13735

cycling performance in full cells coupled with lithium titanate anodes.[26] We expect further improvement in the cycle life with increased degree of cation disordering in $LiNi_{0.5}Mn_{1.5}O_4$. Our results, which clarify the relation between the cycle life and phase evolution, may also aid in understanding the superior cycling stability of $LiFePO_4$ olivine.[18,19] Recently it has been observed that under certain conditions $LiFePO_4$ goes through non-equilibrium solid-solution reactions, rather than the previously recognized phase transformations.[39,40] Besides reducing the particle size,[18,30,39] suppressing phase transformations could be another approach to enable smooth electrochemical reactions and long cycle life.

To summarize, by comparing the stress patterns in situ and phase evolution in a model system of disordered and ordered $LiNi_{0.5}Mn_{1.5}O_4$ spinels with identical chemical composition and film thickness (1 μm), we found that distinct reaction paths cause negligible difference in the overall stress patterns but significantly different cracking behaviors and cycling performances: 95% capacity retention for disordered $LiNi_{0.5}Mn_{1.5}O_4$ and 48% capacity retention for ordered $LiNi_{0.5}Mn_{1.5}O_4$ after 2000 cycles. The extended solid-solution region with suppressed phase transformation is attributed to the superior electrochemical performance of disordered spinel. The relationship between the materials chemistry and its performance found in this work provide the foundation for rationally designing or optimizing electrode materials with long-time performance. In order to substantially improve the reversibility of intercalation-type cathodes and achieve long cycle life, the electrode materials should be engineered to extend the reaction path through stablilzed or metastabilized solid-solution reactions.

■ ASSOCIATED CONTENT

Supporting Information

Experimental methods and data. The Supporting Information is available free of charge on the ACS Publications website at DOI: 10.1021/jacs.5b06178.

■ AUTHOR INFORMATION

Corresponding Authors

*Xingcheng.xiao@gm.com
*dudneynj@ornl.gov

Notes

The authors declare no competing financial interest.

■ ACKNOWLEDGMENTS

J.L., N.J.D., and C.L. acknowledge the support from U.S. Department of Energy (DOE), Office of Science, Basic Energy Sciences, Materials Sciences and Engineering Division. Q. Z., X. X., and Y.T. C. acknowledge the support by the Assistant Secretary for Energy Efficiency and Renewable Energy, Vehicle Technologies Office of the U.S. DOE under contract no. DE-AC02-05CH11231, subcontract no. 7056410 under the Batteries for Advanced Transportation Technologies (BATT) Program. The authors appreciate Rose Ruther and Robert Sacci for their help with Raman and FTIR measurement.

■ REFERENCES

(1) Wu, H.; Chan, G.; Choi, J. W.; Ryu, I.; Yao, Y.; McDowell, M. T.; Lee, S. W.; Jackson, A.; Yang, Y.; Hu, L. *Nat. Nanotechnol.* **2012**, *7*, 310.
(2) Yao, Y.; McDowell, M. T.; Ryu, I.; Wu, H.; Liu, N.; Hu, L.; Nix, W. D.; Cui, Y. *Nano Lett.* **2011**, *11*, 2949.
(3) Xiao, X.; Zhou, W.; Kim, Y.; Gu, M.; Wang, C.; Liu, G.; Liu, Z.; Gao, H. *Adv. Funct. Mater.* **2015**, *25*, 1426.
(4) Zhou, L.; Zhao, D.; Lou, X. D. *Angew. Chem.* **2012**, *124*, 243.
(5) Zhao, K.; Pharr, M.; Vlassak, J. J.; Suo, Z. *J. Appl. Phys.* **2010**, *108*, 073517.
(6) Obrovac, M.; Krause, L. *J. Electrochem. Soc.* **2007**, *154*, A103.
(7) Kovalenko, I.; Zdyrko, B.; Magasinski, A.; Hertzberg, B.; Milicev, Z.; Burtovyy, R.; Luzinov, I.; Yushin, G. *Science* **2011**, *334*, 75.
(8) Wu, M.; Xiao, X.; Vukmirovic, N.; Xun, S.; Das, P. K.; Song, X.; Olalde-Velasco, P.; Wang, D.; Weber, A. Z.; Wang, L.-W. *J. Am. Chem. Soc.* **2013**, *135*, 12048.
(9) Zhou, S.; Yang, X.; Lin, Y.; Xie, J.; Wang, D. *ACS Nano* **2012**, *6*, 919.
(10) Hu, Y. S.; Guo, Y. G.; Dominko, R.; Gaberscek, M.; Jamnik, J.; Maier, J. *Adv. Mater.* **2007**, *19*, 1963.
(11) Zhang, L.; Wu, H. B.; Madhavi, S.; Hng, H. H.; Lou, X. W. *J. Am. Chem. Soc.* **2012**, *134*, 17388.
(12) Woodford, W. H.; Carter, W. C.; Chiang, Y.-M. *Energy Environ. Sci.* **2012**, *5*, 8014.
(13) Croguennec, L.; Palacin, M. R. *J. Am. Chem. Soc.* **2015**, *137*, 3140.
(14) Wang, H.; Jang, Y. I.; Huang, B.; Sadoway, D. R.; Chiang, Y. M. *J. Electrochem. Soc.* **1999**, *146*, 473.
(15) Dokko, K.; Nishizawa, M.; Horikoshi, S.; Itoh, T.; Mohamedi, M.; Uchida, I. *Electrochem. Solid-State Lett.* **2000**, *3*, 125.
(16) Shao-Horn, Y.; Hackney, S.; Kahaian, A.; Kepler, K.; Skinner, E.; Vaughey, J.; Thackeray, M. *J. Power Sources* **1999**, *81*, 496.
(17) Meethong, N.; Huang, H.; Speakman, S. A.; Carter, W. C.; Chiang, Y. M. *Adv. Funct. Mater.* **2007**, *17*, 1115.
(18) Nishijima, M.; Ootani, T.; Kamimura, Y.; Sueki, T.; Esaki, S.; Murai, S.; Fujita, K.; Tanaka, K.; Ohira, K.; Koyama, Y. *Nat. Commun.* **2014**, *5*, 4553.
(19) Zaghib, K.; Dontigny, M.; Guerfi, A.; Charest, P.; Rodrigues, I.; Mauger, A.; Julien, C. *J. Power Sources* **2011**, *196*, 3949.
(20) Wang, C.; Wu, H.; Chen, Z.; McDowell, M. T.; Cui, Y.; Bao, Z. *Nat. Chem.* **2013**, *5*, 1042.
(21) Marks, T.; Trussler, S.; Smith, A.; Xiong, D.; Dahn, J. *J. Electrochem. Soc.* **2011**, *158*, A51.
(22) Myung, S.-T.; Hitoshi, Y.; Sun, Y.-K. *J. Mater. Chem.* **2011**, *21*, 9891.
(23) Chen, X.; Xu, W.; Xiao, J.; Engelhard, M. H.; Ding, F.; Mei, D.; Hu, D.; Zhang, J.; Zhang, J.-G. *J. Power Sources* **2012**, *213*, 160.
(24) Wang, L. P.; Li, H.; Huang, X. J.; Baudrin, E. *Solid State Ionics* **2011**, *193*, 32.
(25) Shaju, K. M.; Bruce, P. G. *Dalton Trans.* **2008**, 5471.
(26) Ariyoshi, K.; Yamato, R.; Makimura, Y.; Amazutsumi, T.; Maeda, Y.; Ohzuku, T. *Electrochemistry* **2008**, *76*, 46.
(27) Li, J.; Ma, C.; Chi, M.; Liang, C.; Dudney, N. J. *Adv. Energy Mater.* **2015**, *5*, 1401408.
(28) Kim, J.-H.; Myung, S.-T.; Yoon, C.; Kang, S.; Sun, Y.-K. *Chem. Mater.* **2004**, *16*, 906.
(29) Manthiram, A.; Chemelewski, K.; Lee, E.-S. *Energy Environ. Sci.* **2014**, *7*, 1339.
(30) Woodford, W. H.; Carter, W. C.; Chiang, Y.-M. *J. Electrochem. Soc.* **2014**, *161*, F3005.
(31) Hu, M.; Pang, X.; Zhou, Z. *J. Power Sources* **2013**, *237*, 229.
(32) Ariyoshi, K.; Iwakoshi, Y.; Nakayama, N.; Ohzuku, T. *J. Electrochem. Soc.* **2004**, *151*, A296.
(33) Lee, E.; Persson, K. A. *Energy Environ. Sci.* **2012**, *5*, 6047.
(34) Lee, E.; Persson, K. A. *Chem. Mater.* **2013**, *25*, 2885.
(35) Sethuraman, V. A.; Chon, M. J.; Shimshak, M.; Srinivasan, V.; Guduru, P. R. *J. Power Sources* **2010**, *195*, 5062.
(36) Mukhopadhyay, A.; Tokranov, A.; Sena, K.; Xiao, X.; Sheldon, B. W. *Carbon* **2011**, *49*, 2742.
(37) Arai, H.; Sato, K.; Orikasa, Y.; Murayama, H.; Takahashi, I.; Koyama, Y.; Uchimoto, Y.; Ogumi, Z. *J. Mater. Chem. A* **2013**, *1*, 10442.
(38) Li, D.; Zhou, H. *Mater. Today* **2014**, *17*, 451.
(39) Liu, H.; Strobridge, F. C.; Borkiewicz, O. J.; Wiaderek, K. M.; Chapman, K. W.; Chupas, P. J.; Grey, C. P. *Science* **2014**, *344*, 1252817.
(40) Sharma, N.; Guo, X.; Du, G.; Guo, Z.; Wang, J.; Wang, Z.; Peterson, V. K. *J. Am. Chem. Soc.* **2012**, *134*, 7867.

DOI: 10.1021/jacs.5b06178
J. Am. Chem. Soc. 2015, 137, 13732−13735